## Cume 365, R. Walterbos

This cume is based on the paper "HI Asymmetries in the Isolated Galaxy CIG 292", published in the 2011 ApJ letters, 739, L27, by Portas etal. Use of calculators is allowed for direct calculations, not for re-calling formulae. A sheet with physical constants is attached.

Anticipated passing grade: 70%. All (sub) questions are 5 pts each. Maximum score is 60 pts.

- 1a. The paper refers to a previous single dish HI observation of this object with the 43 m Green Bank single dish telescope. It cites this telescope as having a beam of 20'. Show this.
- b. Given the beam size, how could a single dish observation be used, as it was apparently, to infer that the galaxy is asymmetric, given that its HI angular extent is only 7' or so (Figure 2)? What asymmetry is measured exactly, and how does this refer to the galaxy's spatial structure?
- 2. In sections 2 and 3, the authors discuss some details of the EVLA observations.
- a. Table 1 lists a quantity called the "primary beam". What is that (not the number, but in words)?
- b. Show that the channel spacing of 15.625 kHz corresponds to 3.32 km/s.
- c. "Continuum subtraction was performed using 10 channels on either side of the velocity range covered by the target that were found to be free from line emission." Why is this step necessary? What could this continuum emission be that they are talking about?
  - d. What is meant with "The cube was cleaned down to a flux threshold of..." What is CLEAN? Why is it necessary?
  - e. The last line in Table 1 expresses the rms noise as  $1.25 \, \text{mJy/beam}$ . It then expresses this noise in terms of a temperature ( $T_B$ ) in Kelvin. What do we call this temperature? Show how you would convert a unit of mJy/beam to Kelvin.
  - f. On page 3: "....the interferometers possibly missed a small fraction of the low-level, extended emission". Why would this happen with interferometric observations?
  - 3a. What is an "SA(s)b" galaxy? (Get at least 3 of the 4 letters right for full credit)
  - b. Consider Figure 4 and the discussion in the paper related to that. What is a "warped disk"? What would Figure 4a look like if the disk were not warped? (Sketch it).
  - c. The paper discusses possible origins of the HI asymmetry, and introduces a concept of HI relaxation time, for which they cite a value of  $10^8$  yrs. Why would a disk that is asymmetric in HI and in isolation possibly reduce its asymmetry on this time scale?
  - d. Show that interactions with possible companions (see section 1, page 2) would indeed be on longer time scales.

Symbol	Meaning	Value
Speed of light in vacuum $h=2\pi h$ Planck's constant $h=h/2\pi$ Rationalized Planck's constant  Boltzmann's constant  Elementary charge of an electr  Electron rest mass  Gravitational constant  Avogadro's number  a. m. u. = u Atomic mass unit  Fine-structure constant  Electron charge to mass ratio  Rem  Rydberg constant  Bohr radius  Compton wavelength	Speed of light in vacuum Planck's constant Rationalized Planck's constant Boltzmann's constant Elementary charge of an electron Electron rest mass Gravitational constant Avogadro's number Atomic mass unit Fine-structure constant Electron charge to mass ratio Rydberg constant Bohr radius Compton wavelength Classical electron'radius	2.997924562(11) × $10^{10}$ cm s <sup>-1</sup> 6.626196(50) × $10^{-27}$ erg s 1.0545919(80) × $10^{-27}$ erg s 1.380622(59) × $10^{-16}$ erg K <sup>-1</sup> 4.803250(21) × $10^{-10}$ esu 9.109558(54) × $10^{-28}$ g 6.6732(31) × $10^{-8}$ dyn cm <sup>2</sup> g <sup>-2</sup> 6.022169(40) × $10^{23}$ mole <sup>-1</sup> 1.660531(11) × $10^{-24}$ g 7.297351(11) × $10^{-3}$ 5.272759(16) × $10^{17}$ esu g <sup>-1</sup> 1.09737312(11) × $10^{-9}$ cm 2.4263096(74) × $10^{-10}$ cm
o=e <sup>4</sup> /(mc <sup>2</sup> ) R 7 7 1.u. wc 4	Gas constant Stefan-Boltzmann constant Thomson cross section	2.817939(13) × $10^{-13}$ cm 8.31434(35) × $10^7$ erg $\mathring{K}^{-1}$ mole <sup>-1</sup> 5.66961(96) × $10^{-5}$ erg cm <sup>-2</sup> s <sup>-1</sup> $\mathring{K}^{-4}$ 6.652453(62) × $10^{-25}$ cm <sup>2</sup> 1.49597892(1) × $10^{13}$ cm 3.0856(1) × $10^{18}$ cm 9.4605 × $10^{17}$ cm = 6.324 × $10^4$ a. u. 1.989(2) × $10^{33}$ g 6.9598(7) × $10^{10}$ cm

# - XII Preface

Symbol	Meaning	Value	
	Solar luminosity One electron volt associated wavelength associated wavenumber associated frequency associated energy associated temperature	$3.826(8) \times 10^{33} \text{ erg s}^{-1}$	
<i>L</i> ⊙ 1 e.V.		12,396.3 × 10 <sup>-8</sup> cm 8067.1 cm <sup>-1</sup> 2.41838 × 10 <sup>14</sup> Hz 1.60184 × 10 <sup>-12</sup> erg 11,605.9 °K	

to the digits in parenthesis following each quoted

雅光红。

# H1 ASYMMETRIES IN THE ISOLATED GALAXY CIG 292

ANTÓNIO PORTAS<sup>1</sup>, TOM C. SCOTT<sup>1</sup>, ELIAS BRINKS<sup>2</sup>, ALBERT BOSMA<sup>3</sup>, LOURDES VERDES-MONTENEGRO<sup>1</sup>, VOLKER HEESEN<sup>2</sup>, DANIEL ESPADA<sup>4</sup>, SIMON VERLEY<sup>5</sup>, JACK SULENTIC<sup>1</sup>, CHANDREYEE SENGUPTA<sup>1,6</sup>, E. ATHANASSOULA<sup>3</sup>, AND MIN YUN<sup>7</sup>

Instituto de Astrofísica de Andalucía (CSIC), Glorieta de Astronomía s/n, 18008 Granada, Spain

<sup>2</sup> Centre for Astrophysics, University of Hertfordshire, Hatfield, Herts AL10 9AB, UK

3 Laboratoire d'Astrophysique de Marseille (LAM), UMR6110, CNRS/Université de Provence/CNRS, Technopôle de Marseille Etoile,
38 rue Frédéric Joliot Curie, 13388 Marseille CEDEX 13, France

<sup>4</sup> National Astronomical Observatory of Japan (NAOI), 2-21-1 Osawa, Mitaka, Tokyo 181-8588, Japan
 <sup>5</sup> Departamento de Física Teórica y del Cosmos, Facultad de Ciencias, Universidad de Granada, Spain
 <sup>6</sup> Calar-Alto Observatory, Centro Astronómico Hispano Alemán, C/Jesús Durbán Remón, 2-2 04004 Almeria, Spain

Department of Astronomy, University of Massachusetts, 710 North Pleasant Street, Amherst, MA 01003, USA Received 2011 April 18; accepted 2011 June 21; published 2011 August 29

### ABSTRACT

We present Expanded Very Large Array (EVLA) D-array observations of the 21 cm line of neutral hydrogen (H<sub>I</sub>) of CIG 292, an isolated SA(s)b galaxy at a distance of  $\sim$ 24.3 Mpc. From previous H<sub>I</sub> single dish observations the galaxy was known to have a mildly asymmetric H<sub>I</sub> profile ( $A_{\text{flux}} = 1.23 \pm 0.3$ ). Our EVLA observations show there is  $\sim$ 12% more H<sub>I</sub> projected south of the optical center (approaching velocities) than in the north (receding velocities), despite the H<sub>I</sub> extending  $\sim$ 16% further to the north than the south. The H<sub>I</sub> projected within the optical disk must have been perturbed within the H<sub>I</sub> relaxation time ( $\sim$ 10<sup>8</sup> yr) which implies that this cannot have been caused by any of the three nearest companions, as their distance ( $\sim$ 0.5 Mpc) is too large. Neither H<sub>I</sub>-rich companions nor tidal tails were found within our field of view and velocity range covered. Our kinematical data suggest that the inner part harbors an oval distortion whereas the outer regions show signs of a modest warp. The mild asymmetry in the H<sub>I</sub> global profile thus actually masks stronger asymmetries in the two-dimensional distributions of gas and star-forming regions in this galaxy. Since the galaxy is isolated, this must predominantly be due to processes related to its formation and secular evolution.

Key words: galaxies: individual (NGC 2712=CIG 292=UGC4708) - galaxies: kinematics and dynamics - galaxies: spiral - galaxies: structure

Online-only material: color figure

### 1. INTRODUCTION

Galaxy evolution and the resulting z = 0 properties of galaxies depend on the environment they find themselves in. In order to quantify the effect of environment ("nurture") on their morphology, structure, nuclear activity, star formation properties, etc., one needs a well-defined sample of galaxies that are minimally perturbed by other galaxies to provide a baseline of what are thought to be unperturbed (or pure "nature") objects. The AMIGA (Analysis of the Interstellar Medium of Isolated GAlaxies; Verdes-Montenegro et al. 2005; http://amiga.iaa.es) project provides a statistically significant sample of the most isolated galaxies. It is a refinement of the original Catalogue of Isolated Galaxies (CIG; Karachentseva 1973). Galaxies in the AMIGA sample have not been involved in a major tidal interaction within the last ~3 Gyr (Verdes-Montenegro et al. 2005). Quantification of the strength of tidal interactions with neighboring minor companions and the local number density is available for all galaxies in the AMIGA sample (Verley et al. 2007a, 2007b). The AMIGA project has clearly established that the most isolated galaxies have different physical properties, even compared to what are generally considered field samples, in terms of their morphology (asymmetry, concentration),  $L_{FIR}$ , the radio-FIR correlation, rate of active galactic nuclei, or H1 asymmetry (Verdes-Montenegro et al. 2010 and references therein).

Despite having much lower rates of H 1 and optical asymmetry than galaxies in denser environments (Durbala et al. 2008; Espada et al. 2011a), some galaxies in the AMIGA sample

show appreciable asymmetry. Espada et al. (2011a) studied the H<sub>I</sub> profiles of a sample of 166 AMIGA galaxies using an H<sub>I</sub> asymmetry parameter  $A_{\rm flux}$  defined as the ratio between the receding and approaching sides of the single dish profile. They found the distribution of this parameter to be well described by the right half of a Gaussian distribution, with only 2% of the sample having an asymmetry parameter in excess of  $3\sigma$  ( $A_{\rm flux} > 1.39$ , meaning a 39% excess of flux in one-half of the spectrum). They did not find any correlation between the H<sub>I</sub> asymmetry parameter and minor companions, measured both as the tidal force (one-on-one interactions) and in terms of the number density of neighboring galaxies. In contrast, field galaxy samples deviate from a Gaussian distribution and have higher (10%–20%) rates of asymmetry (Espada et al. 2011a).

To investigate the causes of asymmetry in the absence of major interactions we are carrying out resolved H I studies of a sample of AMIGA galaxies with the Expanded Very Large Array (EVLA), covering a representative range of H I asymmetry parameters ( $A_{\rm flux}=1.05$  to 1.25). For example, Espada et al. (2005) presented H I VLA D-configuration results of the asymmetric galaxy CIG 96, with Espada et al. (2011b) giving results of further C-array observations of this galaxy. CIG 96 has a large and asymmetric H I envelope ( $R_{\rm HI}/R_{25}=3.5$ ), which partly coincides with faint UV emission with a more regular distribution. The kinematics of this H I envelope shows an area of non-circular motions, which could not be attributed to a major interaction.

Here we present the results of EVLA H I mapping of CIG 292 (NGC 2712) which has an  $A_{\rm flux}=1.23\pm0.30$ , and can be

considered as intermediate between symmetric and asymmetric objects such as CIG 96.

We ascertained once more that CIG 292 is an isolated galaxy. Despite it being listed as part of a group (Tully et al. 2008; Makarov & Karachentsev 2011), only three potential companions have similar recession velocities to CIG 292 but their projected distances are large (58', 62', and 67', thus all of order 0.5 Mpc). CIG 292 turns out to be isolated according to the criteria used by Karachentseva (1973), with local number density and tidal strength characteristics falling within the limits of the bona fide AMIGA sample ( $\eta_k = 1.668$ ,  $Q_{\text{Kar}} = -3.106$ ; Verley et al. 2007b). No H1-rich (dwarf) companions were detected within the 32' region mapped by the EVLA primary beam either. Any current tidal effect is therefore negligible and any past interaction would have been at least 3 Gyr ago.

The neutral hydrogen component of CIG 292 has previously been observed with the Westerbork Synthesis Radio Telescope (WSRT) by Krumm & Shane (1982), and with single dish telescopes by Huchtmeier & Richter (1985) and Springob et al. (2005). CIG 292 is particularly interesting since the H<sub>I</sub> disk is significantly more extended than the optical one (see Section 3.1), and faint optical emission is found at large radius as well (Koopmann & Kenney 2006).

Section 2 gives details of the observations, with the results in Section 3 and discussion and concluding remarks in Section 4. We calculate the distance to the galaxy, based on the observed recession velocity and corrected for Virgo-flow, to be 23.4 Mpc which implies an angular scale where 1' corresponds to  $\sim$ 7 kpc.

### 2. HIOBSERVATIONS

Observations of CIG 292 were obtained using 26 antennas of the NRAO<sup>8</sup> EVLA in D-configuration on 2010 April 25 (Project ID: AE175). The primary calibrator 3C147 (assumed flux density of 22.5 Jy) was observed at the beginning of the run; it was also used as bandpass calibrator. Interspersed with the source, the secondary calibrator J0834+5534 (with a derived flux density of  $8.80 \pm 0.017$  Jy) was observed. In total 3.2 hr were spent on source with both polarizations recorded. CIG 292 was observed across a spectral bandwidth of 4 MHz (corresponding to ~800 km s<sup>-1</sup>), centered at a frequency of 1411.65 MHz, at a frequency resolution of 15.625 kHz (3.32 km s<sup>-1</sup>). In Table 1, we provide some general properties of the galaxy, as well as the principal parameters of the observational setup.

The data were correlated using the new EVLA WIDAR correlator, and the data reduction was performed using CASA (Common Astronomy Software Applications) version 3.02. For guidance we followed the spectral line tutorials available online at the CASA Web site.9 The data reduction was carried out on one of the nodes of the cluster of the Centre for Astrophysics Research at the University of Hertfordshire.

The EVLA observations were carried out at night, avoiding any possible issues related to solar interference. Antenna position corrections were applied to antennas 12 and 22. We edited (flagged) the data based on the average of the inner 150 channels (from the 256 available). We also decided to omit all data from antennas 9, 14, 17, and 23 at this stage as their L-band receivers had not been upgraded and their visibilities presented values one order of magnitude lower than average.

15.625 Lt

Table 1 General Properties and Observational Setup for CIG 292

Parameter	Value	
Object	CIG 292	
α (J2000) <sup>a</sup>	8h59m30s53	
δ (J2000) <sup>a</sup>	44°54′51″5	
Morphological type <sup>b</sup>	SA(s)b	
Optical inclination <sup>b</sup>	58°	
log L <sub>B</sub> <sup>c</sup> ⊃re	9.77 $\log \mathcal{L}_{\odot}$	
Instrument	EVLA	
Observing date	2010 Apr 25	
Configuration	D-array	
Project ID	AE175	
Primary calibrator	3C147	
Secondary calibrator	J0834+5534	
Central velocity	1842 km s <sup>-1</sup>	
FWHM of primary beam	32'	
Total bandwidth	4.0 MHz	
Number of channels	256	
Channel spacing	15.625 kHz (3.32 km s <sup>-1</sup> )	
FWHM of synthesized beam	46"× 42"	
Time on source	3.2 hr	
rms noise	1.25 mJy beam <sup>-1</sup> (0.4 K T <sub>B</sub> )	

#### Notes.

Calibration of the spectral line data was performed by first solving for phase corrections to the 3C147 scan followed by deriving the bandpass complex gains on this calibrator. Amplitude and phase solutions for the flux calibrator and phase calibrator (J0834+5534) were derived from the average of channels 50 to 200 (i.e., on a quasi-continuum data set). After first inspection, a further iteration of flagging and calibration was applied, including flagging of bad visibilities related to the target. Continuum subtraction was performed using 10 channels on either side of the velocity range covered by the target that were found to be free from line emission.

Imaging of CIG 292 was performed using CASA's standard cleaning algorithm. We produced a cube using the Briggs robust weighting scheme (Briggs 1995) where we found robust = 0.5to be a good compromise between spatial resolution (which results in a beam size of  $46" \times 42"$ ) and sensitivity. The cube was cleaned down to a flux threshold of  $3\sigma$  (3.75 mJy beam<sup>-1</sup>).

The cube was subsequently transferred into AIPS (version 31DEC11) in order to restore the velocity information to the header since observations were taken at a fixed frequency. We fixed the center of the band at a velocity of 1842 km s<sup>-1</sup>. We separated genuine emission from noise following the conditional blanking method employed by Walter et al. (2008). A data cube convolved to 75" resolution was used to mask regions of emission that were above  $2\sigma$  rms noise over three consecutive velocity channels. As a final step, the zero- and first-order moment maps (total surface brightness and velocity field) were created using AIPS task XMOM. Both the data cube and the moment 0 map were corrected for primary beam attenuation.

### 3. EVLA H1 RESULTS

### 3.1. H I Integrated Map and Spectra

We present in Figure 1 the EVLA H1 integrated spectrum for CIG 292 and that of the single dish profile obtained by

The National Radio Astronomy Observatory is a facility of the National Science Foundation, operated under cooperative agreement by Associated Universities, Inc. 1411.65 MHz

http://casaguides.nrao.edu/

<sup>&</sup>lt;sup>a</sup> Leon & Verdes-Montenegro (2003).

<sup>&</sup>lt;sup>b</sup> Durbala et al. (2008).

<sup>&</sup>lt;sup>c</sup> D. Espada et al. (2011, private communication).

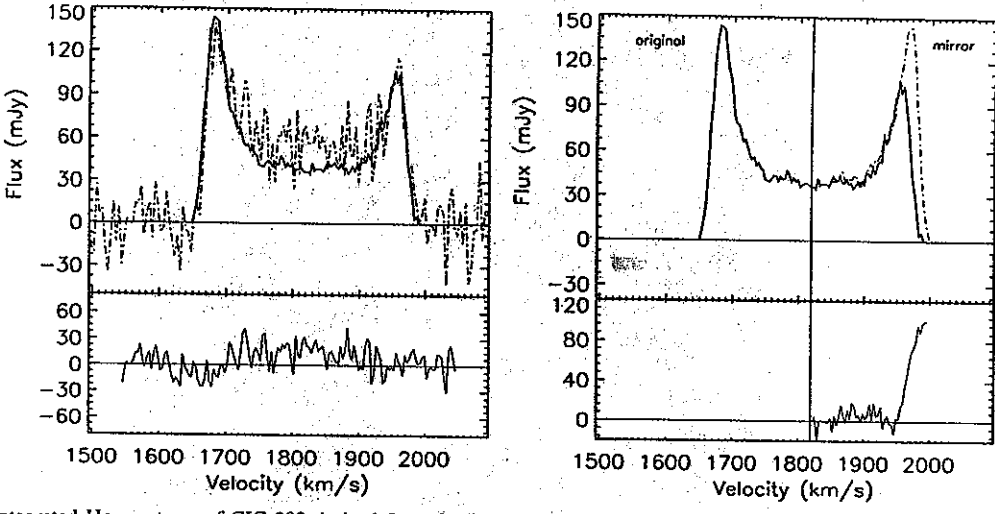


Figure 1. Left panel: integrated H<sub>1</sub> spectrum of CIG 292 derived from the EVLA data (solid line). Emission is detected in the velocity range 1650 km s<sup>-1</sup> to 1950 km s<sup>-1</sup>. The dashed dotted line represents the 43 m Green Bank single dish. H<sub>1</sub> profile retrieved from Springob et al. (2005). Right panel: integrated EVLA H<sub>1</sub> spectrum of CIG 292 where the approaching portion of the spectrum has been flipped around V = 1818 km s<sup>-1</sup> (vertical line) and overplotted (dash-dotted line) for comparison with the receding portion of the spectrum. The lower panels show the difference between each pair of spectra.

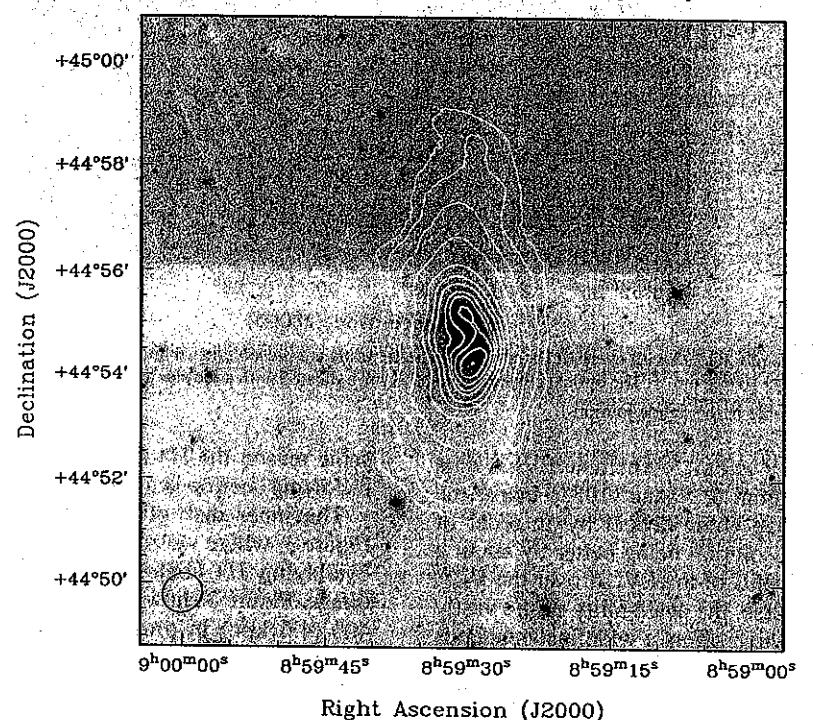


Figure 2. H1 contours of CIG 292 on an SDSS r-band image. Contours are drawn at 0.5, 1.0, 1.2, 3.7, 6.2, 7.6, 8.5, 9.5, 10.0, 10.6, 11.4, and  $12.1 \times 10^{20}$  at cm<sup>-2</sup>. The beam size is shown in the bottom left corner of the image.

Springob et al. (2005) using the 43 m Green Bank (formerly known as 140 ft) radio telescope with a beam of 20'. We also present in the same figure the difference between both spectra. We measured an integrated EVLA flux of 19.0 Jy km s<sup>-1</sup> which translates to an H<sub>I</sub> mass of  $2.5 \times 10^9 M_{\odot}$  assuming optically thin emission. This value is in good agreement with previous interferometric observations of this object performed with the WSRT (Krumm & Shane 1982) of 20.1 Jy km s<sup>-1</sup> ( $2.6 \times 10^9 M_{\odot}$ ) and the flux retrieved by Springob et al. (2005) obtained with the 43 m telescope of 22.26 Jy km s<sup>-1</sup>, the interferometers possibly missed a small fraction of low-level, extended emission. In that context it is interesting to note where the main differences between Green Bank and EVLA spectra originate (see Figure 1).

We recover most of the flux in the regions of the peaks where

the emission in individual channels is most compact. It is in the central velocity channels (between 1700 km s<sup>-1</sup> and 1900 km s<sup>-1</sup>) of the galaxy where the H  $_{\rm I}$  is possibly more extended since on average we underestimate the single dish flux by some 20%.

We also present in Figure 1, a folded profile determined down to 20% of the peak level, by flipping the emission around a velocity of 1818 km s<sup>-1</sup>. This shows that most of the asymmetry is coming from the highest velocities in the profile, in the 1950 km s<sup>-1</sup> to 2000 km s<sup>-1</sup> range, corresponding to the northern side of the galaxy.

In Figure 2 we show the H I column density map of CIG 292 as contours overlaid on the SDSS r-band image. The galaxy has an extended H I disk with a diameter of  $\sim$ 46 kpc (6.5) measured

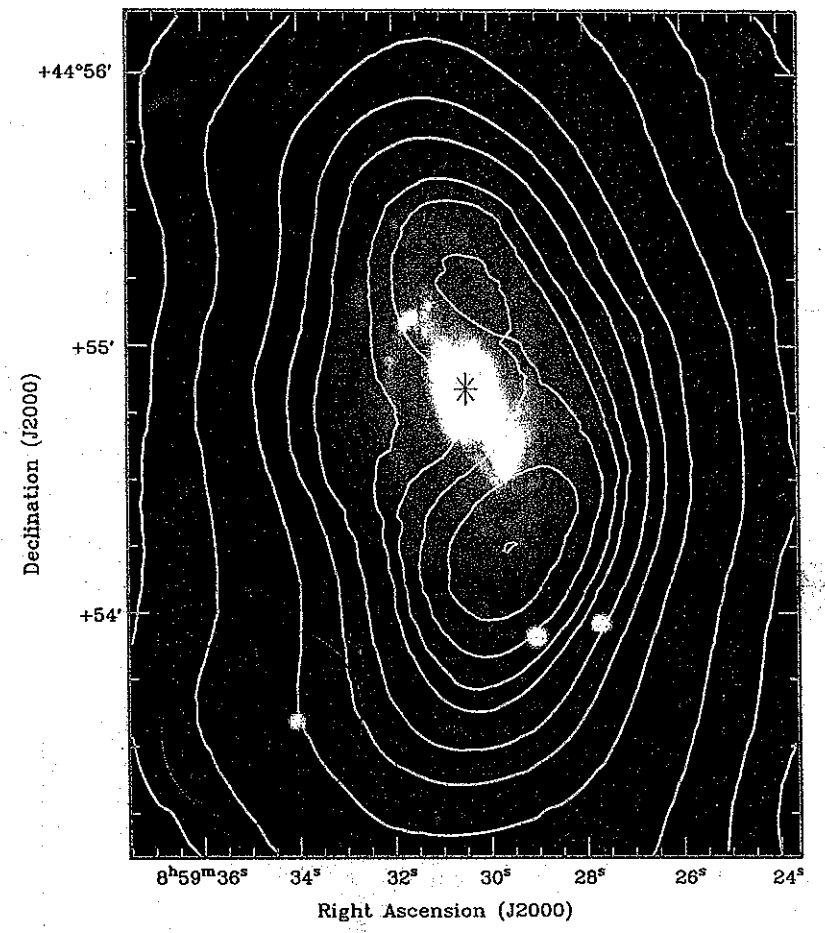


Figure 3. Optical SDSS urg composite of CIG 292 with overlaid H1 contours. The contours are presented as white solid lines and correspond to levels of 1.2, 3.7, 6.2, 7.6, 8.5, 9.5, 10.0, 10.6, 11.4, and 12.1  $\times$  10<sup>20</sup> at cm<sup>-2</sup>. The optical center of the galaxy is indicated with a red star and the beam is shown in the bottom left of the image. (A color version of this figure is available in the online journal.)

at a column density of  $5 \times 10^{19}$  at cm<sup>-2</sup>. The new EVLA data are vastly superior to the Krumm & Shane (1982) maps, the total H<sub>I</sub> surface brightness map going deeper by an order of magnitude, and the velocity resolution being better by about a factor of five. The specific benefits of the EVLA over the VLA for this kind of work is, of course, the availability of the vastly superior WIDAR correlator which offers a wide instantaneous velocity range which opens up the possibility to search for companions within a large volume around a target while maintaining high velocity resolution to study any object thus detected.

Down to the noise level of  $3.5 \times 10^{19}$  at cm<sup>-2</sup> (a  $3\sigma$  detection across five channels or 16.5 km s<sup>-1</sup> which corresponds to the typical line width of H1 at a velocity dispersion of 7 km s<sup>-1</sup>), the galaxy measures 3.6 (25 kpc) to the south and 4.3 (30 kpc) to the north, making it lopsided. The extended nature of the HI structure in the north can be traced across 10 consecutive individual velocity channels (~32 km s<sup>-1</sup>), indicating that it is part of the galaxy. The  $R_{25}$ -to- $R_{\rm H_{1}}$  ratio is  $\sim$ 2.2 assuming an  $R_{25}$  of 1.5 (LEDA) and our  $R_{\rm H_1}$  of 3.25 measured at 5 × 10<sup>19</sup> at cm<sup>-2</sup>. This falls within the typical range of optical to H<sub>I</sub> extent from the study by Broeils & Rhee (1997) of  $1.7 \pm 0.5$ . At the current H1 resolution, no details such as spiral arms or evidence for a bar can be discerned in our H I data. Because up to 20% of the total flux is missing in some of the channel maps due to the lack of short-spacings, which mainly affects the extended structure, our RH1 and RH1-to-R25 ratio are lower limits. For the same reason the H<sub>I</sub> mass-to-luminosity ratio presented in the following section is a lower limit.

The inner disk of the galaxy is shown in more detail in Figure 3, where we zoom in on the central region of the galaxy, overlaying H1 contours on an SDSS u, g, and r composite image. Figure 3 shows that the column density peak is offset by 40'' (4.6 kpc) in projection to the SW of the optical center (marked with a star in the figure), with the higher density contours forming an arc-like structure along the western side of the galaxy.

## 3.2. Kinematics

We present in Figure 4 the velocity field of CIG 292. The galaxy shows regular rotation throughout most of its disk. The isovelocity contours at the outskirts (beyond 2'.5) are however twisted, symptomatic of a warped disk. Initially the twist is point symmetric and clockwise, but in the far north (beyond 3'.6 or 25 kpc) the position angle (P.A.) twists back, counterclockwise.

A position-velocity (PV) diagram along the major axis of the galaxy (P.A. =  $-5^{\circ}$ ) is shown in Figure 4 (bottom panel). We trace the southern side here out to  $\sim$ 3'.6 and the northern side to  $\sim$ 4'.3. The PV diagram shows steeply rising rotation, unresolved by the beam, within the inner part (up to  $\sim$ 1' in diameter) followed by flat rotation out to the last measured point on either side. Márquez et al. (2004) using optical long-slit spectroscopy confirm the steep rise in the gas component, the peak velocity being reached within 10" (1.2 kpc).

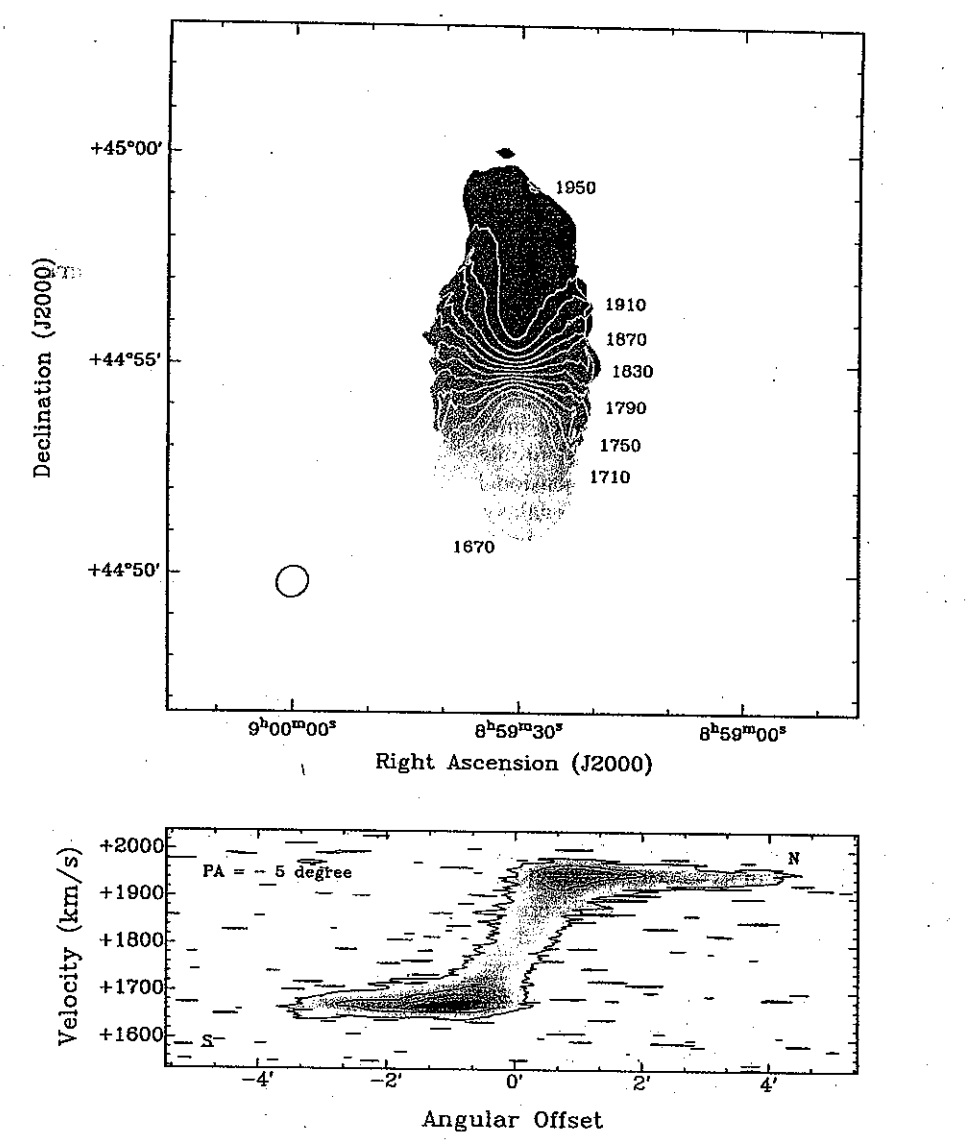


Figure 4. Top panel: velocity field of CIG 292 with velocity contours superimposed. Velocity contours range from 1670 km s<sup>-1</sup> (southern half) to 1950 km s<sup>-1</sup> (northern half) in steps of 20 km s<sup>-1</sup>. We only label every other contour. Bottom panel: position-velocity diagram along the major axis taken at a P.A. of ~5°. Contours are at a level of 0.25, 0.4, 1.4, 2.4, 3.4, and 4.4 mJy beam<sup>-1</sup>.

Assuming circular rotation and the inclination of 58° from LEDA, we can use our data to find a dynamical mass for CIG 292. At the last point of the rotation curve at 30.1 kpc (measured at a column density of  $3.5 \times 10^{19}$  at cm<sup>-2</sup>) we measure an indicative rotation velocity of 120 km s<sup>-1</sup> or an intrinsic velocity of 140 km s<sup>-1</sup>. Using  $M_{\rm dyn} = 0.76RV^2/G$  gives a dynamical mass of  $1.1 \times 10^{11} M_{\odot}$ . This implies an  $M/L_{\rm B} = 18.9$ . We find an  $M_{\rm H}/L_{\rm B} = 0.4$ . This makes it underluminous for its Hubble type (Roberts & Haynes 1994). Further data at higher angular resolution are needed to provide a detailed mass model.

## 4. DISCUSSION AND CONCLUDING REMARKS

The H<sub>I</sub> results show that CIG 292 has an asymmetric H<sub>I</sub> distribution, extending farther north than south, with a twist in the outer parts suggestive of a slightly warped atomic gas disk. Even so, the H<sub>I</sub> extension is at the side where there is the *least* H<sub>I</sub> in the integrated profile. Thus, the asymmetry in the H<sub>I</sub> global profile is partly masking a stronger asymmetry in the

two-dimensional distribution, as already suggested by Espada et al. (2011a).

A closer look at the available optical images in NED shows a system of faint optical arms (Koopmann & Kenney 2006). Using ellipse fitting, the P.A. at those radii is about  $-3^{\circ}$ , in reasonable agreement with the P.A. of the major axis indicated by the kinematics, which is about  $-6^{\circ}$  between 2.5 and 4.0 arcmin radius. The more central parts of the galaxy have a P.A. of about  $+5^{\circ}$ , which indicates that the galaxy there has an oval shape, consistent with the fact that the kinematical major and minor axes at those radii are not perpendicular (Bosma 1978). Moreover, this oval is seen as an enhancement above the underlying exponential disk (a "lens" component) in the radial luminosity profile presented in Erwin et al. (2008). Such a feature is rather common in early-type spiral galaxies (e.g., Kormendy 1979).

Inspection of available Galaxy Evolution Explorer images,  $H\alpha$  images, and the 8  $\mu$ m image from the Spitzer archive shows that this bright inner region is copiously forming stars, and has asymmetries in the distribution of star-forming regions. This

coincides with the asymmetry in the inner H<sub>I</sub> distribution as noted in Figure 3. These asymmetric distributions within the optical radius must have been perturbed within the relaxation timescale for the high-density gas, i.e., of the order of 108 yr (Boselli et al. 1994). This short relaxation timescale seems to preclude an interaction with any of the three nearest companions as the source of the high-density H I asymmetry.

We can exclude as well an encounter with a companion with a large pericenter distance since this would necessitate a massive companion which is simply not there. Alternatively, the largescale asymmetry may be due to an interaction with a small companion which in the meantime has merged, or to ongoing cold accretion (e.g., Bournaud et al. 2005).

In conclusion, our new EVLA data on this galaxy have revealed that the mild asymmetry in the H<sub>I</sub> global profile actually hides stronger asymmetries in the two-dimensional distributions of gas and of the star-forming regions in this galaxy. Our data indicate that the central bright parts of the optical disk form an oval distortion, with a P.A. that is different from that of the faint optical disk and the bulk of the H I disk. In the northern part there is an extension, which is not necessarily in the same plane as the outer disk.

As for the causes of such asymmetries in isolated galaxies, the oval distortion comes naturally from a bar instability in the disk (e.g., Athanassoula 2010). The asymmetry in the neutral gas distribution could be related to ongoing accretion of the neutral gas from the cosmic web at angles forcing the outer HI disk to be warped w.r.t. the optical disk (e.g., Jiang & Binney 1999). Alternatively, it could be due to an m = 1 instability. Data at higher angular resolution will be necessary to study the kinematics of the inner bright regions, in order to discern the dynamical causes of the asymmetries.

This work has been supported by the research projects AYA2008-06181-C02 from the Spanish Ministerio de Ciencia e Innovación, the Junta de Andalucía (Spain) grants P08-FQM-4205, FQM-0108, TIC-114, and FP7-ICT-2009-6.

The NASA Extragalactic Database, NED, is operated by the Jet Propulsion Laboratory, California Institute of Technology, under contract with the National Aeronautics and Space Administration.

We acknowledge the usage of the HyperLeda database (http://leda.univ-lyon1.fr).

Funding for the SDSS and SDSS-II has been provided by the Alfred P. Sloan Foundation, the Participating Institutions, the National Science Foundation, the U.S. Department of Energy, the National Aeronautics and Space Administration, the Japanese Monbukagakusho, the Max Planck Society, and the Higher Education Funding Council for England. The SDSS

Web site is http://www.sdss.org/. The SDSS is managed by the Astrophysical Research Consortium for the Participating Institutions. The Participating Institutions are the American Museum of Natural History, Astrophysical Institute Potsdam, University of Basel, University of Cambridge, Case Western Reserve University, University of Chicago, Drexel University, Fermilab, the Institute for Advanced Study, the Japan Participation Group, Johns Hopkins University, the Joint Institute for Nuclear Astrophysics, the Kavli Institute for Particle Astrophysics and Cosmology, the Korean Scientist Group, the Chinese Academy of Sciences (LAMOST), Los Alamos National Laboratory, the Max-Planck-Institute for Astronomy (MPIA), the Max-Planck-Institute for Astrophysics (MPA), New Mexico State University, Ohio State University, University of Pittsburgh, University of Portsmouth, Princeton University, the United States Naval Observatory, and the University of Washington.

### REFERENCES

Athanassoula, E. 2010, in ASP Conf. Ser. 421, Galaxies in Isolation: Exploring Nature Versus Nurture, ed. L. Verdes-Montenegro et al. (San Francisco, CA: ASP), 157

Boselli, A., Gavazzi, G., Combes, F., Lequeux, J., & Casoli, F. 1994, A&A, 285,

Bosma, A. 1978, PhD thesis, Univ. of Groningen

Bournaud, F., Combes, F., & Semelin, B. 2005, :-

, 364, L18

, 160,

, 436,

Briggs, D. S. 1995, PhD thesis, New Mexico Tech.

Broeils, A. H., & Rhee, M.-H. 1997, A&A, 324, 877

Durbala, A., Sulentic, J. W., Buta, R., & Verdes-Montenegro, L. 2008, 390, 881

Erwin, P., Pohlen, M., & Beckman, J. E. 2008, A&A, 135, 20

, 442, 455

Espada, D., Bosma, A., Verdes-Montenegro, L., et al. 2005,

Espada, D., et al. 2011a, A&A

Espada, D., et al. 2011b, ApJ, in press

Huchtmeier, W. K., & Richter, O.-G. 1985, A&A, 149, 118 Jiang, I.-G., & Binney, J. 1999, MARKAS, 303, L7

Karachentseva, V. E. 1973, Soobshch. Spets. Astrofiz. Obs., 8, 3

Koopmann, R. A., & Kenney, J. D. P. 2006, Appl., 162, 97

Kormendy, J. 1979, ApJ, 227, 714

Krumm, N., & Shane, W. W. 1982, A&A, 116, 237

Leon, S., & Verdes-Montenegro, L. 2003, Adv., 411, 391

Makarov, D., & Karachentsev, I. 2011, Marie et 412, 2498

Márquez, I., Durret, F., Masegosa, J., et al. 2004,

Roberts, M. S., & Haynes, M. P. 1994, ARAMA, 32, 115

Springob, C. M., Haynes, M. P., Giovanelli, R., & Kent, B. R. 2005, 149

Tully, R. B., Shaya, E. J., Karachentsev, I. D., et al. 2008, 676, 184 Verdes-Montenegro, L., Del Olmo, A., & Sulentic, J. (ed.) 2010, ASP Conf. Ser. 421, Galaxies in Isolation: Exploring Nature Versus Nurture (San Francisco,

Verdes-Montenegro, L., Sulentic, J., Lisenfeld, U., et al. 2005, 443

Verley, S., Leon, S., Verdes-Montenegro, L., et al. 2007b,

, 470, Verley, S., Odewahn, S. C., Verdes-Montenegro, L., et al. 2007a,

Walter, F., Brinks, E., de Blok, W. J. G., et al. 2008,

Cume 365, suggested solutions.

- 1a. This asks for the usual formula for the beam (PSF) of a telescope, 1.2 lambda/Diameter.
- 1b. The beam of the single dish indeed more than covers the entire galaxy, but the asymmetry can be inferred from the spectrum. A galaxy disk will have one side approaching us, the other side receding. thus, the difference in the HI spectrum between the blue- and red-shifted (with respect to the systemic velocity) halves of the spectrum can show an asymmetry in HI content between the two galaxy halves.
- 2a. The primary beam refers to the beam size of a single dish in the interferometer array. This determines the field of view for the interferometer. This is to be distinguished from the "synthesized beam" which refers to the actual beam ("PSF") of the interferometer.
- 2b. Simply equate (delta\_freq)/freq. to (delta\_v)/(speed of light).

Here delta\_freq is the spectral resolution stated (15.625 kHz), and freq=1420 MHz.

2c. The telescope does not only collect the 21-cm line emission, but any continuum emission that falls in the bandpass. This continuum emission varies only slowly across the narrow total bandwidth, and contributes roughly equal to all individual velocity channels. It needs to be removed from the line emission to estimate the true HI signal. The "line-free channels" are identified by inspecting the HI data cube for channels that no longer have HI emission, which is likely to occur at the two velocity extremes of the band-pass.

The sources of the continuum emission include synchrotron and bremsstrahlung emission from background radio sources and the galaxy itself.

2d. An interferometer only covers part of the baseline range that a single dish (of the size of the largest spacing between interferometer dishes) would cover. There are many gaps in the baseline space. The consequence of the gaps is that the "synthesized beam" of the interferometer has various side lobes, and a negative bowl at large angular scales caused by missing the shorted spacings in the baseline plane.

The synthesized beam of an interferometer is the theoretical response to a point source at the center of the field. The synthesized beam is used to CLEAN the map, using the following steps:

- 1. Identify the location of the highest peak in the map.
- 2. Multiply the synthesized beam, which has peak 1, with a scale factor that is equal to a fraction of the peak flux value found in step 1.
- 3. Subtract from each pixel in the map the scaled synthesized beam, shifted to the position of that highest peak.
- 4. Save the delta-function which describes this one "clean component" at the relevant map location.
- 5. Repeat steps 1 through 4 till reaching the noise level.
- 6. Convolve the map of the saved delta-functions with a "clean beam" (usually the central part of the synthesized beam).

7. Add the residual noise map from step 5 to the output of step 6. This is the final map of the interferometer. Ideally, this process corrects all the artifacts introduced by the missing baselines.

2e. The temperature asked for is the Brightness temperature. It is the temperature a black body would have at the frequency in question to match the observed intensity at that frequency.

mJy/beam is a unit of surface brightness, or intensity, as is brightness temperature.

The two can be related to each other:

In radio regime, the Planck function is always in the Rayleigh-Jeans tail, ( $hv \ll kT_B$ ) or  $B_v(T_B) = 2 v^2 k T_B/c^2$ .

Calculate the beam size (this is the size of the synthesized beam) in steradian. Use e.g. pi (ab/4) where a and b are the FWHM dimensions given in the paper.

A mJy is a flux unit (I gave the value on the board), convert to erg cm<sup>-2</sup> s<sup>-1</sup> Hz<sup>-1</sup>

A unit of mJy/beam can then be related to a temperature T<sub>B</sub>.

I was not looking for the exact answer, but the method.

2f. An interferometer cannot observe a "zero meter baseline" since you can't put the dishes closer together than the diameter of one of them. This hole at the short spacings causes a negative bowl in the synthesized beam, and hence also in the entire map. The missing zero spacing in particular has an important consequence. The sky distribution is the Fourier Transform of the phases and gains recorded by the interferometer. According to the FT theorems, the FT of a function in one domain at the value 0, is equal to the integral from - to + infinity over the function in the other domain. If an interferometer cannot get a value at the zero meter baseline, this means that the net flux in the sky domain of the interferometer map is actually zero.

3a. SA(s)b

S= spiral

A = not barred

(s) = spiral arms start all the way in the center; (r) would mean there is an inner ring from which the spiral arms start.

b refers to the bulge size and the tightness of the winding of the spiral arms.

3b. A warped disk is a disk that is not in one plane but one that curves outside the plane while remaining thin. The way this shows up in the velocity field diagram is as a twisting of the symmetry line of the velocity contours. A flat disk that has no warp would have a straight line bisecting the velocity contours.

3c. This is in fact a very confusing section in the paper. The paper the authors refer to does not say anything about a relaxation time, but talks about ram pressure stripping and tidal interactions as sources of the HI asymmetry. The students did not have that information, so I graded this question liberally. My own thoughts are that the authors should have referred to a rotational period of gas in a rotating disk; with a flat rotation curve, the winding that will occur will wipe out asymmetries between disk halves. Some students interpreted it as a Jean's collapse or free-fall time.

3d. The typical time for interaction with companion galaxies is determined by the distance and typical velocities in a group. The latter is of order hundreds of km/s, not thousands. Given the stated distances of the companion galaxies, the time scales are much longer than  $10^8$  years.